

Interface Material for Enhancement of Weldability between Dissimilar Materials: 405 Ferritic Stainless Steel and 705 Zr Alloy by Friction Welding Process

K. Koundinya¹, A. Chennakesava Reddy²

¹PG student Department of Mechanical Engineering, JNTUH College of Engineering, Kukatpally, Hyderabad – 500 085, Telangana, India

²Professor, Department of Mechanical Engineering, JNTUH College of Engineering, Kukatpally, Hyderabad – 500 085, Telangana, India

Abstract: The current work was aimed to assess three joints, namely vee-joint, square joint and plain joint, used for improving weldability of dissimilar 705 Zr alloy and 405 ferritic stainless steel materials with an interface material between them by continuous drive friction welding. Three joints were evaluated for their strength, heat affected zone and metal flow across the weld joints. The vee-joint was found to be better as compared to plain and square joints.

Keywords: 705 Zr alloy, 405 ferritic stainless steel, interface material, frictional pressure, vee joint, square joint, plain joint, frictional time, rotation speed, friction welding

1. Introduction

In the developing of new technologies, the use of joints between dissimilar materials has considerably increased [1]. In continuous drive friction welding, one of the workpieces is attached to a motor driven unit while the other is restrained from rotation as showed in figure 1a. The motor driven workpiece is rotated at a predetermined constant speed. The workpieces to be welded are forced together and then a friction force is applied as shown in figure 1b. Heat is generated because of friction between the welding surfaces. This is continued for a predetermined time as showed in figure 1c. The rotating workpiece is halted by the application of a braking force. The friction force is preserved or increased for a predetermined time after the rotation is ceased (figure 1d).

only from the different coefficients of thermal expansion, but also from the distinct hardness values of the dissimilar materials to be joined. The microstructural evolution of the interface of 5052 Al alloy/304 stainless steel depends on thermo-chemical interactions between the two materials [2]. Joint and edge preparation is very important to produce distortion free welds. The solid-state diffusion is slow in the wider joints [3]. The intermetallic compounds can change the micro hardness near the joint interface of dissimilar metals [4]. Therefore, friction welding of dissimilar metals needs to be eased by ensuring that both the workpieces deform similarly. In this context, a research work was carried out with alternative joint designs for the joining interface of mild steel/austenite stainless steel, through a systematic study of incorporating uniform material flow at the interface [5, 6].

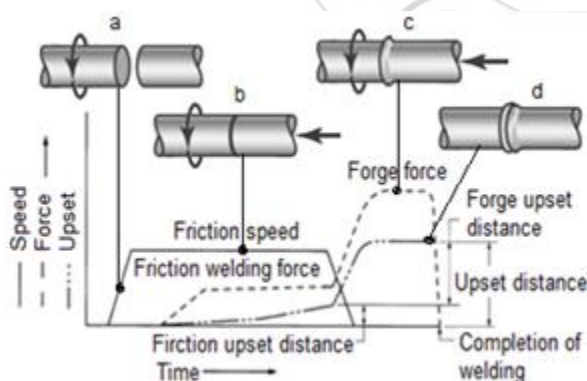


Figure 1: Friction welding.

Several studies of the joining of aluminum alloys to steels by friction welding have been reported. With friction welding, joints are possible between not only similar materials, but also dissimilar materials can be welded. The foremost difference between the welding of similar materials and that of dissimilar materials is that the axial movement is unequal in the latter case whilst the similar materials experience equal movement along the common axis. This problem arises not

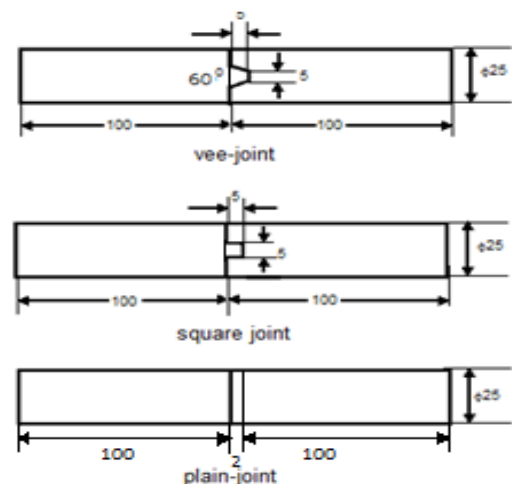


Figure 2: Design of joints

Based on the earlier experimental work [5, 6] for various joint designs, the current work was proposed to investigate the weldability of friction welding process for dissimilar materials: 705 Zr-alloy and 405 ferritic stainless steel (FSS) with interface material between them using finite element

method approach. The designs of three weld joints namely vee joint, square joint and plain joint are shown in figure 2.

2. Materials and Methods

In order to predict the performance of three proposed joints, 705 Zr-alloy and 405 ferritic stainless steel cylindrical bars of 25mm diameter and length of 100mm were considered. Also, to increase the weldability, pure aluminum sheet which is compatible to both 705 Zr-alloy and 405 ferritic stainless steel is used as an interface material. The levels chosen for the controllable process parameters are summarized in table 1. Each of the process parameters was chosen at three levels. The orthogonal array (OA), L9 was preferred to carry out experimental and finite element analysis (FEA). The obligation of parameters in the OA matrix is given in table 2.

Table 1: Control parameters and levels

Factor	Symbol	Level-1	Level-2	Level-3
Frictional pressure, MPa	A	40	45	50
Frictional time, sec	B	4	6	8
Speed, rpm	C	1200	1600	2000
Type of joint	D	Plain	Square	Vee

Table 2: Orthogonal array (L9) and control parameters

Treat No.	A	B	C	D
1	1	1	1	1
2	1	2	2	2
3	1	3	3	3
4	2	1	2	3
5	2	2	3	1
6	2	3	1	2
7	3	1	3	2
8	3	2	1	3
9	3	3	2	1

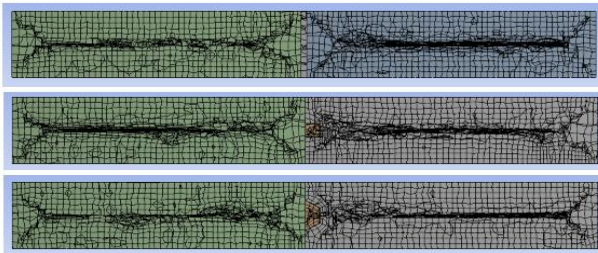


Figure 3: Discretization of weld rods and aluminum interface

In the finite element analysis of friction welding [7-14], first the transient thermal analysis was performed keeping the 705 Zr alloy rod, pure aluminum sheet stationary and the 405 FSS rod in rotation. Figure 3 depicts the discretization of rods and interface. The coefficient of friction 0.2 was applied at the interface of the 705 Zr alloy, pure aluminum sheet and 405 FSS rods. The convection heat transfer coefficient was applied on the surface of two rods and aluminum sheet. The heat flux calculations were imported from ANSYS APDL commands and applied at the interface of three materials to be welded. The temperature distribution was estimated. The Thermal analysis was coupled with the static structural analysis. For the structural analysis the rotating (405 FSS) rod was brought to stationary and the forging pressure was applied on the 705 Zr alloy rod along the longitudinal axis.

The 705 Zr alloy rod was allowed to move in the axial direction.

3. Results and Discussion

The statistical Fisher's test was carried out to find the acceptability of process parameters at 90% confidence level.

3.1 Effect of Process Parameters on Temperature

Table – 3 presents the ANOVA (analysis of variation) summary of temperature distribution. The frictional pressure (A), frictional time (B), rotational speed (C) and type of joint (D) would contribute, respectively, 9.42%, 14.67%, 37.36% and 38.55% in the total variation of the welding temperature.

Table 3 ANOVA summary of temperature

Source	Sum 1	Sum 2	Sum 3	SS	v	V	F	P
A	9411.8	11137.8	12250	681746.9	2	340873	130714.15	9.42
B	9025.6	11212.2	12561.8	1061519.5	2	530759	203529.51	14.67
C	7892.2	11369.2	13538.2	2703967	2	1351983	518442.76	37.36
D	14225.6	12898455	32799.6	2789942.5	2	1394971	534927.19	38.55
e				23.47	9	2.607	1.00	0
T	40555.2	12932174	71149.6	7237199.3	17			100

Note: SS is the sum of square, v is the degrees of freedom, V is the variance, F is the Fisher's ratio, P is the percentage of contribution and T is the sum squares due to total variation.

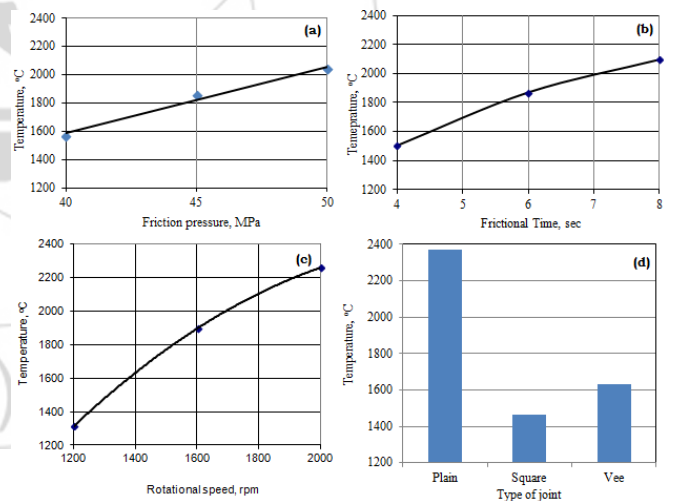


Figure 4: Effect of process parameters on temperature

The temperature was directly proportional to the frictional pressure, frictional time and rotating speed as shown in figure 4. The temperature developed in the plain joint was higher than that of square and vee joints. High temperature gradients resulted at the weld interfaces due to high frictional pressure and rotating speed on rods. The welding conditions of trial 9 would generate the highest temperature (2936°C) and trial 6 would produce the lowest temperature (1266°C) in the rods (figure 5).

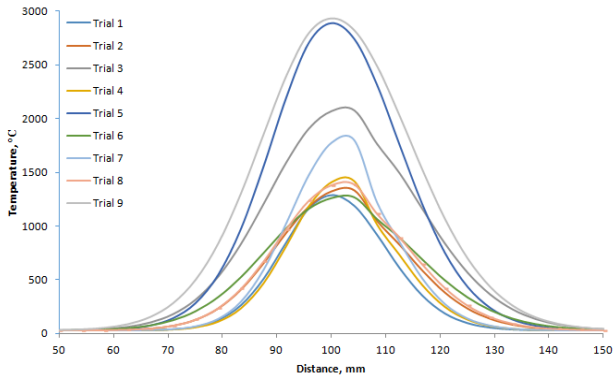


Figure 5: Temperature distribution during different trials

the HAZ for trials 5 and 6 were, respectively, 696 MPa and 414 MPa as shown in Figure 8.

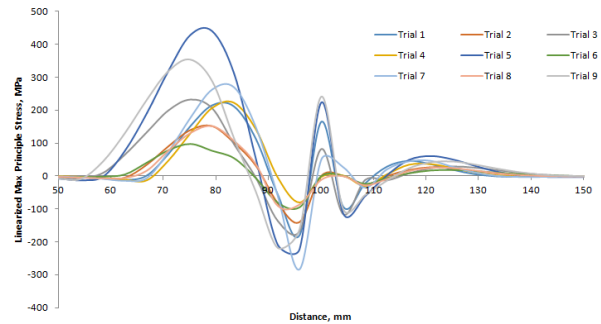


Figure 7: Linearized maximum principle stress in weld rods

3.2 Effect of Process Parameters on Effective Stress

The ANOVA summary of the equivalent stress is given in table 4. The contributions were 17.31%, 4.77%, 43.71% and 34.19%, respectively, attributed to frictional pressure (A), frictional time (B), rotational speed (C) and type of joint (D) towards the total variation of effective stress.

Table 4: ANOVA summary of the effective stress

Source	Sum I	Sum 2	Sum 3	SS	v	V	F	P
A	2836.76	3171.4	3406.96	27366.7	2	13683	5870.00	17.31
B	2965.06	3215.04	3235.02	7542.64	2	3771	1617.85	4.77
C	2705.82	3095.78	3613.52	69113.5	2	34556	14824.44	43.71
D	3582.34	1303383.4	9415.12	54069.41	2	27034	11597.57	34.19
E				20.9796	9	2.33	1.00	0.02
T	12089.98	1312865.6	19670.62	158113.23	17			100

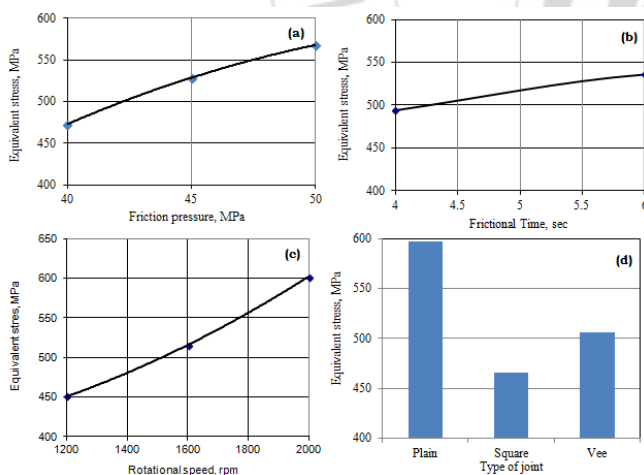


Figure 6: Effect of process parameters on effective stress

The frictional pressure, frictional time and rotational speed would increase the equivalent stress induced in the weld rods as shown in figure 6. It can also be observed from figure 7 that the stress induced in the grain refined region of heat affected zone (HAZ) was higher in all the welds than that in the parent metal. For plain joint the HAZ was observed on either side of interface; whereas for square and vee joints the HAZ was observed around the periphery shape of the joints (figure 8). The equivalent stress induced in the plain joint was higher than the rest of the joints. The stress induced in

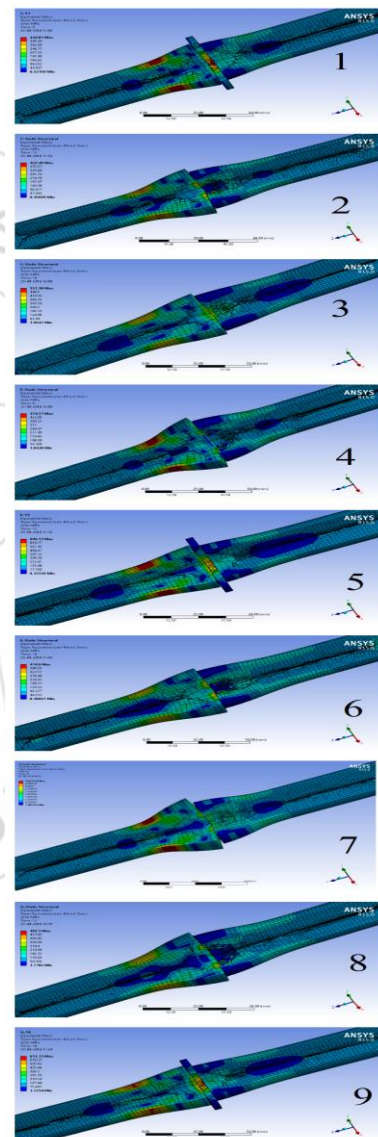


Figure 8: Effect of process parameters on effective stress

3.3 Effect of Process Parameters on Bulk Deformation

The ANOVA summary of the bulk deformation is given in table 5. The major contributions were of type of joint (57.43%), rotational speed (18.98%), frictional time (18.98%) and frictional pressure and type of joint (6.17%) towards variation in the bulk deformation.

Table 5 ANOVA summary of the bulk deformation

Source	Sum 1	Sum 2	Sum 3	SS	v	V	F	P
A	2.47	3.10	3.32	0.07	2	0.035	32.46	6.17
B	2.08	3.13	3.68	0.22	2	0.11	102.01	18.98
C	2.07	3.17	3.64	0.22	2	0.11	-102.01	18.98
D	4.58	0.68	8.88	0.67	2	0.335	310.66	57.43
E				-0.0097051	9	0.0010783	1.00	-1.56
T	11.20	10.08	19.52	1.1702949	17			100

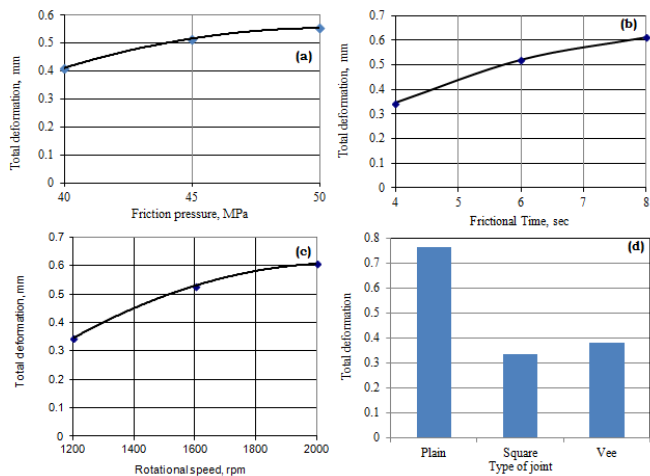


Figure 9: Effect of process parameters on bulk deformation.

The bulk deformation was found to be minimum for 4 sec of frictional time and rotational speed of 1200 rpm (figure 9b). The extruded shape was asymmetric, as shown in figure 10. The tendency of flange formation was higher with 405 FSS than with 705 Zr alloy. The axial shortening on the 405 FSS side was more than that on 705 Zr alloy side. Consequently, the 405 FSS was moved outward forming the flange at the interface. This is also due to the fact that melting point of 405 FSS is lower than that of 705 Zr alloy.

4. Conclusion

This study shows that the weldability of 705 Zr alloy and 405 ferritic stainless steel is highly enhanced by introducing an interface material which is compatible to both the alloys. The stresses induced in the plain joint was higher than vee and square joints. The vee joint imparts good strength at the joint because of mechanical interlocking and equal bulk deformation.

5. Acknowledgment

The authors wish to thank University Grants Commission (UGC), New Delhi for the support of this work.

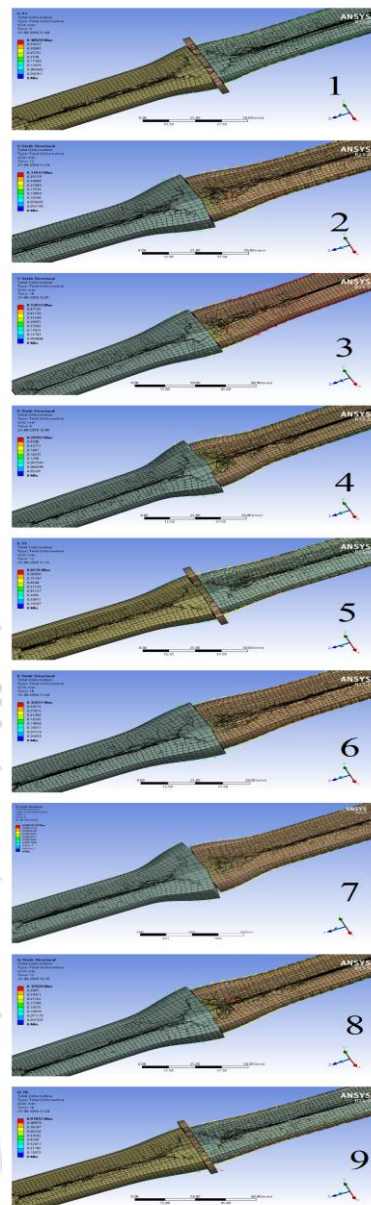


Figure 10: Effect of process parameters on bulk deformation

References

- [1] V. I. Vill, friction welding of metals, AWS New York, 1962.
- [2] S. Fukumoto, H. Tsubakino, K. Okita, M. Aritoshi, T. Tomita, Friction welding process of 5052 aluminum alloy to 304 stainless steel. Mater Sci Techno 15, pp.1080-1086, 1990.
- [3] A. C. Reddy, K. Ravaivarma, and E. Thirupathi Reddy, A study on the effects of joint and edge preparation to produce cost reduction and distortion free welds, National Welding Seminar, IIT-Madras, 07-09th January, 2002, pp.51-55.
- [4] A. C. Reddy, Fatigue Life Evaluation of Joint Designs for Friction Welding of Mild Steel and Austenite Stainless Steel, International Journal of Science and Research, 4(2), pp. 1714-1719, 2015.
- [5] A. C. Reddy, Fatigue Life Prediction of Different Joint Designs for Friction Welding of 1050 Mild Steel and 1050 Aluminum, International Journal of Scientific & Engineering Research, 6(4), pp. 408-412, 2015.

- [6] A. C. Reddy, Evaluation of Parametric Significance in Friction Welding Process for AA7020 and Zr705 Alloy using Finite Element Analysis, International Journal of Emerging Technology and Advanced Engineering, 6(2), pp. 40-46, 2016.
- [7] A. C. Reddy, Weldability of Friction Welding Process for AA2024 Alloy and SS304 Stainless Steel using Finite Element Analysis, International Journal of Engineering Research and Application, 6(3), pp. 53-57, 2016.
- [8] A. C. Reddy, Finite Element Analysis of Friction Welding Process for AA7020-T6 and Ti-6Al-4V Alloy: Experimental Validation, International Journal of Science and Research, 4(8), pp. 947-952, 2015.
- [9] A. C. Reddy, Evaluation of parametric significance in friction welding process for AA2024 and Zr705 alloy using finite element analysis, International Journal of Engineering Research & Technology, 5(1), pp. 84-89, 2016.
- [10] A. C. Reddy, Analysis of welding distortion in seam and skip arc weldings using finite element method, International Journal of Mechanical Engineering Research & Development, 1(1), pp.12-18, 2011.
- [11] V. Srija and A. C. Reddy, Finite Element Analysis of Friction Welding Process for 2024Al Alloy and UNS C23000 Brass, International Journal of Science and Research, 4(5), pp. 1685-1690, 2015.
- [12] T. Santhosh Kumar and A. C. Reddy, Finite Element Analysis of Friction Welding Process for 2024Al Alloy and AISI 1021 Steel, International Journal of Science and Research, 4(5), pp.1679-1684, 2015.
- [13] A. Raviteja and A. C. Reddy, Finite Element Analysis of Friction Welding Process for UNS C23000 Brass and AISI 1021 Steel, International Journal of Science and Research, 4(5), pp. 1691-1696, 2015.
- [14] Y. Lekhana, A. Nikhila, K. Bharath, B. Naveen, A. Chennakesava Reddy, Weldability Analysis of 316 Stainless Steel and AA1100 Alloy Hollow Tubes using Rotational Friction Welding Process, International Journal of Science and Research, 5(5), pp. 622-627, 2016